Mar. Sci. Tech. Bull. (2024) 13(4): 262-271
e–ISSN: 2147–9666
info@masteb.com

dergipark.org.tr/en/pub/masteb
www.masteb.com
DOI: 10.33714/masteb.1549709

Marine Science and Technology Bulletin

PRENSIP
https://prensip.gen.tr/

RESEARCH ARTICLE

Hydrodynamic performance improvement of a tirhandil yacht by Stern form modifications

Sertaç Bulut[1*]

[1] *Izmir Katip Celebi University, Department of Naval Architecture and Marine Engineering, Izmir, Türkiye*

ARTICLE INFO

Article History:
Received: 14.09.2024
Received in revised form: 04.10.2024
Accepted: 14.10.2024
Available online: 18.10.2024

Keywords:
Stern form modification
Computational fluid dynamics
Hydrodynamics
Turbulence models
Yachts

ABSTRACT

This paper presents a comprehensive investigation to improve the hydrodynamic performance of a Tirhandil hull form by modification efforts on the stern region. The form improvement approach combines computational fluid dynamics (CFD) methods with computer-aided design (CAD) systems. The design process for the reference and modified models was carried out by using CAD systems. The hydrodynamic characteristics of the reference hull form were evaluated by employing CFD methods and it was determined that form improvements should be concentrated on the stern region. The modification process was conducted by considering constraints on the design variables in the stern region and the main dimensions of the reference model. A grid independence study was performed to evaluate various grid structures to determine the optimal mesh configuration for the numerical analyses. The SST k-Omega turbulence model was used for the numerical analyses to simulate turbulence structure around the hull form. Achieving around a 13.4% reduction in the total resistance coefficient, the modified model also exhibited decreased wave amplitudes, smoother wave transitions, and a significant reduction or cancellation of shoulder and stern waves.

Please cite this paper as follows:

Bulut, S. (2024). Hydrodynamic performance improvement of a tirhandil yacht by Stern form modifications. *Marine Science and Technology Bulletin*, *13*(4), 262-271. https://doi.org/10.33714/masteb.1549709

Introduction

Yachts have long held a significant place in maritime culture, offering not only cultural and economic value but also substantial touristic benefits. Their influence on local economies is substantial, particularly in industries such as tourism, boat building, and marine services, where they generate income and employment. Beyond their cultural and economic impact, yachts contribute meaningfully to environmental sustainability efforts within the maritime sector. In recent years, the focus on improving yacht designs has gained momentum, driven by the need for both economic efficiency and environmental protection. These modifications are essential, as they enhance hydrodynamic performance, resulting in reduced fuel consumption and lower emissions.

* Corresponding author
E-mail address: sertac.bulut@ikc.edu.tr (S. Bulut)

This is particularly important given the rising global demand for greener shipping practices, which seek to balance operational cost savings with environmental responsibility. Therefore, modifying yacht designs plays a crucial role in meeting both economic and environmental goals, helping the industry adapt to the challenges of sustainable development more efficiently.

Tirhandil yachts, an important part of our maritime culture, hold significant potential for form improvement efforts with their traditional and unique designs. Tirhandils, known for their rich historical backgrounds and aesthetic forms, are widely used in the Aegean and Mediterranean regions. As one of the oldest boat forms originating from the Aegean, Tirhandils are distinguished by their symmetrical bow and stern design. Tirhandils have found broad applications in the fishing and sponge diving industries of Greece, Italy, and Turkey (Ozen, 2017). The term 'Tirhandil', derived from the Greek word 'trea-kena', meaning 'one-third', emphasizes that these boats have a one-third width-to-length ratio (Koyagasioglu, 2014). Tirhandil boats, with historical roots dating back to ancient times including the Phoenicians, have documented records from as early as 1658 by G. D. Kriezis (Koyagasioglu, 2014; Gür, 2020). According to historian Dentes, the first Tirhandil boats were constructed in the 17th century on the island of Hydra. Used historically for fishing, transportation, and military purposes, 20 Tirhandil boats were part of the Ottoman Navy in 1790 (Gencer, 2001). Production of Tirhandil boats began in Bodrum in the 1950s and by the 1960s, they had also found their place in the waters of Istanbul (Mahmuzlu, 2019). Today, they are also used for private and tourism purposes along the Aegean and Mediterranean coasts. The literature review reveals limited studies on Tirhandils, primarily using semi-empirical methods, and lacking any research focused on form improvements through CFD analyses. When the literature is reviewed, it becomes evident that there are limited studies on Tirhandils, mostly conducted using semi-empirical methods, and no studies have been found that involve form improvements using CFD analyses. Ganos & Loukakis (1986) conducted model tests on Tirhandil-type boat hulls. A limited number of models were used, and the resistance characteristics of Tirhandil boats were examined. Damianidis (1989) studied the production history and main features of various boat types within Greece, including Tirhandils. Turan & Akman (2021) developed parametric models to analyze the hull form characteristics of Bodrum Gulets with round and transom sterns, comparing their hydrostatic and resistance performances. Turan et al. (2021) analyzed the forms of Gulet and Tirhandil boats, presenting their hydrostatic and hydrodynamic characteristics. Turan (2022) compared the hull forms of Tirhandil and Piyade boats, highlighting their performance differences in terms of resistance and deck space utilization. Turan (2023) introduced a parametric design framework for trawler-type motor yachts, providing resistance estimation values using only the LOA in the early stages of the design process. Turan et al. (2024) proposed a conceptual design framework for Tirhandil yachts, focusing on hull form, resistance, and sailing performance.

The modification of hull forms holds the promise of enhancing the flow structures around the yachts and improving resistance characteristics. Traditionally, such modifications were tested using physical models in towing tanks, but with advances in computer technology and Computational Fluid Dynamics (CFD) methods, these processes can now be simulated with greater efficiency and accuracy. However, simulations conducted in the field of form improvement using CFD methods also involve certain challenges, such as the prediction of complex turbulent structures around the form, computational load, accurate boundary condition representation, grid sensitivity, and the coupling of multiple physical phenomena like fluid-structure interaction. Especially the bow and stern regions of the hull present specific challenges due to their high-pressure fluctuations, large wave amplitudes, and higher resistance values. These regions are often the focus of modifications, as they can greatly influence the overall performance of the yacht. Improving the flow and reducing resistance in these regions is essential for enhancing both fuel efficiency and operational performance.

The modification studies of aft hull forms have gained increasing attention in recent years due to the significant impact that the stern shape has on a yacht's hydrodynamic performance. Improvements to the stern region can reduce resistance, improve fuel efficiency, and enhance overall boat performance. Several studies in this area have focused on improving the stern forms using various methods and approaches to achieve better results in terms of hydrodynamic characteristics. Kükner & Mamur (2016) conducted a study exploring the effects of various bow and stern form combinations on vessel resistance, generating 252 different boat models for analysis. Their results showed that the plumb bow form, combined with other optimized stern forms, exhibited the lowest resistance, primarily due to the longer waterline length and improved water separation. Ali & Ali (2016) proposed a novel stern shape concept using radial crenellated-corrugated sections and reverse piezoelectric effects to reduce total forward resistance. Their study demonstrated that this new stern design significantly reduced propeller cavitation, improving overall vessel performance. Song et al. (2018) assessed the impact of stern flaps and interceptors on the drag resistance, trim, and sinkage of a high-speed deep-vee ship using experimental and CFD methods. Results showed that both devices reduced drag resistance, with interceptors performing better at higher speeds and stern flaps at lower speeds, achieving drag reductions of 3–9%. Various studies have also explored the effects of different stern configurations and appendages on total vessel resistance and hydrodynamic performance, yielding significant improvements in resistance reduction and overall performance (Maki et al., 2016; Mansoori & Fernandes, 2016, 2017; Deng et al., 2020; Lena et al., 2021; Song et al., 2024). Duy & Hino (2015) focused on optimizing the transom stern shape to minimize the pressure resistance coefficient using a CFD solver based on the Reynolds-Averaged Navier-Stokes equations. Reductions in pressure resistance of approximately 5–6% were observed, with total resistance reductions of 1.9–2.3%, depending on the test case. Marcu & Robe-Voinea (2024) investigated the stern flow hydrodynamics around a manoeuvring ship by using CFD techniques. Their findings revealed that stern vortices and turbulent flow patterns significantly affect the propeller inflow and contribute to increased ship resistance. Lu et al. (2019) proposed a methodology for the synchronous optimization of bow and stern hull forms across the entire speed range of the KRISO Container Ship (KCS). An average drag reduction of over 4.0% was achieved across various speeds, with the best performance at mid-range Froude numbers. Anggriani & Baso (2020) investigated the performance of a ship by optimizing the stern hull form to match the propeller diameter and engine power for high-speed operations. It was observed that the U-shape stern outperformed the V-shape stern, with reduced total resistance and lower power requirements at a Froude number of approximately 0.22. Mutsuda et al. (2013) conducted a numerical investigation using Computational Fluid Dynamics (CFD) and Particle Image Velocimetry (PIV) to examine the effects of stern part modifications on reducing drag resistance in fishing boats. The study revealed that the optimized designs reduced water resistance by 15–20% compared to the original form, primarily by controlling separated flow and vortex formation around the stern. Baso et al. (2019) examined the effects of stern part improvements on the heave and pitch motions of a fishing boat using a hybrid scheme of Eulerian grid-Lagrangian particles. Stern modifications resulted in a 5% to 10% rise in heave amplitude and a 5% to 9% rise in pitch amplitude, with a more significant impact on heave motion, highlighting the method's effectiveness for preliminary ship design. Several researchers also worked on reducing resistance in the stern part of fishing boats, including studies by Masuya (2007), Karafiath (2012), and Suastika et al. (2017). Solak (2020) focused on optimizing the stern form using a Kriging-based high-fidelity method combined with genetic algorithms to minimize viscous pressure drag. This approach resulted in at least a 5% reduction in viscous pressure drag, improving the hydrodynamic performance of the vessel.

In this study, form modifications were performed, focusing on the stern region to improve the hydrodynamic performance of a Tirhandil hull form. The reference model and modified model were designed using CAD systems. The hydrodynamic characteristics of the reference Tirhandil model were determined through flow simulations using Computational Fluid Dynamics (CFD) methods. Based on the hydrodynamic characteristics of the reference form, it was determined that form improvement efforts should be concentrated on the stern region of the hull form. The modification process was carried out by considering the constraints applied to the design variables defined in the stern region. Additionally, constraints related to the main dimensions of the reference model were also considered in the form improvements. A grid independence study was performed using various grid structures to determine the optimal mesh configuration for the numerical analyses. The SST k-Omega turbulence model was used to simulate the turbulence around the hull form in the numerical analyses. The hydrodynamic characteristics of the reference and modified models were comparatively investigated. The modified model achieved approximately a 13.4% reduction in the total resistance coefficient, featuring reduced wave amplitudes, smoother wave transitions, and a significant reduction or cancellation of shoulder and stern waves. A review of the literature reveals that no previous work has offered such a hydrodynamic performance improvement study on the stern region for Tirhandil yachts. Through the modification process, a unique Tirhandil design with improved hull form characteristics was developed. This research also provides a framework that can guide form optimization studies for sailing yachts.

Material and Methods

Governing Equations

The evaluation of flow patterns in this study is based on the governing Navier-Stokes and continuity equations. The continuity and momentum equations in Cartesian coordinates are formulated as:

$$\frac{\partial \rho}{\partial t} + \frac{\partial (\rho u_i)}{\partial x_i} = 0 \quad (1)$$

$$\rho \left(\frac{\partial u_i}{\partial t} + u_j \frac{\partial u_i}{\partial x_j} \right) = -\frac{\partial P}{\partial x_i} + \mu \frac{\partial^2 u_i}{\partial x_j^2} + f_i \quad (2)$$

In these equations, ρ signifies fluid density, u_i indicates velocity components, P stands for the pressure field, μ is the dynamic viscosity, and f_i represents external forces.

Flow structures and turbulence distribution are modelled using the RANS-based SST k–Omega model (Menter, 1994). The methods of Reynolds averaging and filtering are commonly applied to convert the Navier-Stokes equations into a resolvable form, preventing the direct modelling of smaller turbulent scales. Reynolds averaging divides a flow variable into a mean value, $\bar{\theta}(x,t)$, and a fluctuating component, $\theta'(x,t)$.

$$\theta(x,t) = \bar{\theta}(x,t) + \theta'(x,t) \quad (3)$$

Equation 4 shows the RANS equations derived from the incompressible Navier-Stokes equations.

$$\frac{\partial}{\partial t}(\rho\overline{u_i}) + \frac{\partial}{\partial x_j}(\rho\overline{u_i u_j}) = -\frac{\partial\overline{p}}{\partial x_i} + \frac{\partial}{\partial x_j}\left[\mu\left(\frac{\partial\overline{u_i}}{\partial x_j} + \frac{\partial\overline{u_j}}{\partial x_i}\right)\right] + \frac{\partial R_{ij}}{\partial x_j} \quad (4)$$

In this equation, $\bar{u}_i$ and $\bar{u}_j$ refer to the Reynolds-averaged velocity, and $\bar{p}$ represents the Reynolds-averaged pressure field. The Navier-Stokes and RANS equations differ primarily due to the presence of the Reynolds stress tensor (Equation 5), introduced by the Boussinesq hypothesis (Boussinesq, 1877).

$$R_{ij} = -\rho\overline{u_i u_j} = \mu_t\left(\frac{\partial\overline{u_i}}{\partial x_j} + \frac{\partial\overline{u_j}}{\partial x_i}\right) - \frac{2}{3}k\delta_{ij} \quad (5)$$

RANS-based turbulence models calculate eddy (turbulent) viscosity, μ_t, using different approaches. The SST k-Omega model (Wilcox, 1988) employs a blending function that combines a k-Omega model near the wall with a k-Epsilon model in the outer flow region. This model also incorporates an innovative approach to eddy viscosity, which accounts for the transport of the primary turbulent shear stress. The k-omega model calculates turbulent viscosity based on turbulent kinetic energy (k) and the specific dissipation rate (ω) (Equation 6).

$$\mu_t = \alpha^*\frac{\rho k}{\omega} \quad (6)$$

Numerical Setup

This part outlines the numerical setup employed in the simulations. The flow around the ship hull was modelled using numerical solutions of the continuity and Navier-Stokes equations. The URANS solver was applied, with the finite volume method used to discretize the Navier-Stokes equations. The simulation of turbulent flow structures was achieved using the SST k-Omega model in CFD analyses. Each momentum equation was solved sequentially in the numerical simulations using a segregated flow solver. The solver integrates an algebraic multigrid approach for efficient computation. For spatial discretization of the convection and diffusion terms, a second-order upwind scheme was applied in the governing equations. The discretization of temporal terms in the governing equations was achieved through a first-order unsteady implicit method. ITTC's guidelines (ITTC, 2011) for Reynolds stress models were followed in the simulations, which use a time-step of 0.004 seconds and 10 inner iterations. The free surface effects of a floating ship were modelled using multiphase flow simulation. The Volume of Fluid (VOF) approach was used to represent free surface effects, considering two or more immiscible fluid phases and tracking the interface between them.

The accuracy of the solutions depends heavily on the placement of domain boundaries and the appropriate selection of boundary conditions. The computational domain has boundaries positioned 3 LOA forward from the bow, 8 LOA aft of the stern, 3 LOA on the sides from the symmetry plane, 2 LOA below the keel, and 1 LOA above the deck. ITTC recommendations (ITTC, 2011, 2014) were taken into account when defining the computational domain. For the boundary conditions, velocity inlets were applied at the inlet, top, and bottom surfaces, a pressure outlet was set behind the hull, symmetry conditions were imposed on the sides, and a no-slip condition was used on the hull. Figure 1 provides a visual representation of the computational domain and the boundary conditions.

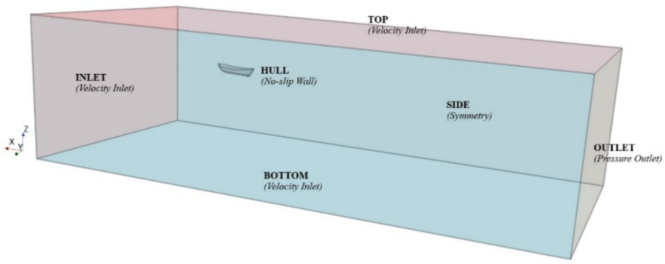

Figure 1. Overview of the computational domain and boundary conditions

The accuracy of fluid flow simulations and the rate of convergence are heavily influenced by the mesh generation process. Mesh quality was enhanced in certain critical regions of the computational domain. Refinement volumes were defined to apply local improvements to the mesh within the domain. Local mesh improvements were concentrated around the hull form, stern, bow, wake region, and free surface. The trimmed cell mesher technique was used to create a robust and efficient mesh structure. According to ITTC recommendations (ITTC, 2011, 2014), 10 prism layers with a 1.2 expansion ratio were employed. To provide the optimal mesh configuration for flow analysis, a grid independence study was performed. The refined regions enabled a gradual and smooth connection between the prism layers and the outer mesh. A y+ value of around 30 was implemented for the SST k-omega model as part of the All y+ wall treatment, providing accurate resolution of the buffer layer and inertial sublayer. Figure 2 presents a detailed presentation of the mesh configuration used in the flow analysis from different viewpoints.

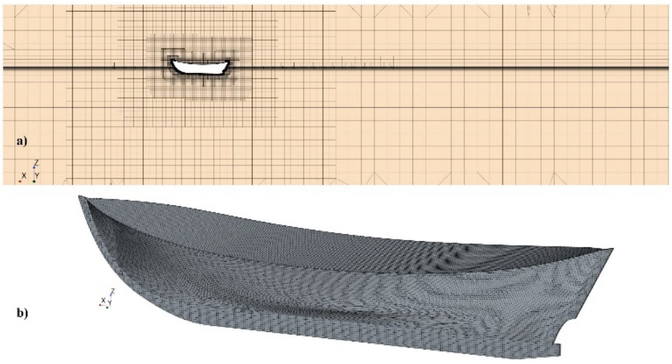

Figure 2. Mesh configuration: a) Side view b) Hull surface

Results and Discussion

Grid Independence Studies

The accurate modelling of the boundary layer, along with satisfying the conditions of turbulence models, is essential for providing precise results in the flow analyses. A proper mesh setup ensures an effective trade-off between accuracy and computational efforts. The GCI method (Celik et al., 2008) was used to assess discretization errors, contributing to establish a suitable mesh configuration. Mesh discretization errors were determined using the total resistance coefficient (C_T) as a reference parameter. The GCI parameters for the coarse, medium, and fine mesh configurations, with 2.4, 1.7, and 1.2 million cells respectively, for the reference model at Froude number of 0.38 were presented in Table 1. The grid refinement factor, *r*, was calculated as the ratio of the finer mesh element size to that of the coarser mesh. As outlined below, the apparent order of accuracy was calculated from the corresponding definitions.

$$p = \frac{1}{\ln(r_{21})} \left| \ln|\varepsilon_{32}/\varepsilon_{21}| + q(p) \right| \tag{7}$$

$$q(p) = \ln\left(\frac{r_{21}^p - s}{r_{32}^p - s}\right) \tag{8}$$

$$s = 1 \times sgn\left(\frac{\varepsilon_{32}}{\varepsilon_{21}}\right) \tag{9}$$

Here, $\varepsilon_{32} = \theta_3 - \theta_2$, $\varepsilon_{21} = \theta_2 - \theta_1$ and θ_k corresponds to the solution on the *kth* grid. A negative ratio $\varepsilon_{32}/\varepsilon_{21} < 0$ are a possible indication of oscillatory convergence (Celik et al., 2008). The following definition was used to derive the extrapolated values:

$$\theta_{ext}^{21} = (r_{21}^p \theta_1 - \theta_2)/(r_{21}^p - 1) \tag{10}$$

θ_{ext}^{32} can also be calculated similarly Equations 11 and 12 were used to calculate the approximate relative error (e_a^{21}) and extrapolated relative error (e_{ext}^{21}), respectively.

$$e_a^{21} = \left|\frac{\theta_1 - \theta_2}{\theta_1}\right| \tag{11}$$

$$e_{ext}^{21} = \left|\frac{\theta_{ext}^{12} - \theta_1}{\theta_{ext}^{12}}\right| \tag{12}$$

The definition for determining the grid convergence index for the fine-to-medium grids is as follows:

$$GCI_{fine}^{21} = \frac{1.25 . e_a^{21}}{r_{21}^2 - 1} \tag{13}$$

Grid refinement progressively decreased the GCI ($GCI_{fine}^{21} < GCI_{med}^{32}$) or the total resistance (R_T). A considerable reduction in GCI from the coarser to the finer grid was achieved, as shown in Table 1. According to the results, the grid-independent solution was almost obtained, and further refining the grid would not lead to substantial changes. Thus, given both accuracy and computational cost, the medium mesh with 1.7 million cells was preferred for the numerical simulations, as indicated by the grid convergence analysis.

Table 1. Parameters of the grid convergence method

GCI Parameters	Values
N_1, N_2, N_3 ($\times 10^6$)	2.4, 1.7, 1.2
G_1, G_2, G_3 ($\times 10^3$)	8.409, 8.575, 9.271
φ_{ext}^{21}	0.84
e_a^{21} (%)	1.97
e_{ext}^{21} (%)	0.62
GCI_{fine}^{21} (%)	0.77
GCI_{med}^{32} (%)	3.18

Comparison With Reference Model and Modified Model

In this section, a detailed comparison of the hydrodynamic characteristics between the reference and modified models was examined. Flow simulations for the reference and modified models were performed at a speed of 4.12 m/s, which corresponds to a Froude number of 0.38, using CFD methods. The numerical analysis covered a comprehensive investigation of resistance results, pressure coefficients, and wave patterns. The simulations were performed through the use of the commercial software STAR-CCM+ (StarCCM+ User Guide, 2023). The computational process was conducted on PC clusters, each featuring 24 Intel Core (64-bit, 3.0 GHz to 5.8 GHz) processors, with funding provided by TUBITAK.

The modified model (MDF) was generated by implementing improvements in the stern region of the reference model (REF) using CAD systems. Design splines were defined on the stern form, and design variables were positioned on these splines (Figure 3). The modification process was performed by considering the constraints applied to these design variables. Constraints are also applied to form characteristics such as draft (T), beam (B), length (L), displacement (∇), and wetted surface area (SW). The dimensional ratios of L/B and B/T for the Tirhandil form were maintained. The variation allowed in displacement and wetted surface area was limited to below 1%. The difference in draft values between the reference model and the modified model is also below 1%. Hydrostatic analyses were conducted for both models, and no significant differences were observed in the changes to the hydrostatic values. Figure 4 presents the hull forms of the reference and modified models in detail.

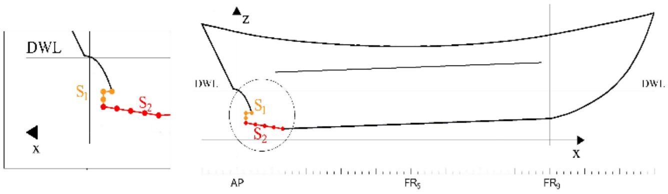

Figure 3. Design splines and design variables

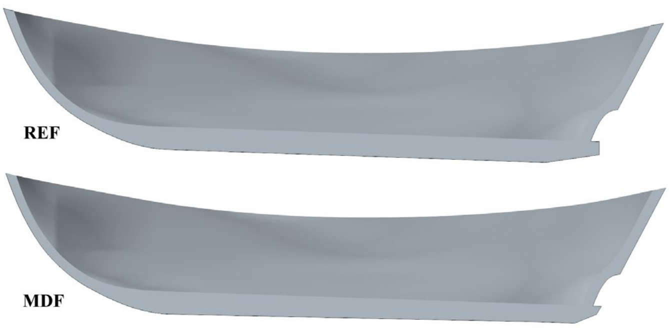

Figure 4. Hull forms of reference and modified models

Turan et al. (2024) conducted field studies on 23 different Tirhandil boats. They created 3D models of the Tirhandils using CAD software, performed engineering analyses on these models to determine the boats' characteristics, and applied regression analyses on the data to determine the design criteria and hull form parameters for Tirhandils. The reference Tirhandil form used in this study was developed based on the data presented in the work of Turan et al. (2024). The general dimensions of the reference model are presented in Table 2.

Table 2. General dimensions of the reference model

Specifications	Reference Model
Waterline length (LWL)(m)	11.41
Waterline width (BWL) (m)	3.53
Draft (m)	1.39
Displacement (tonnes)	11.35

A comparison of the total resistance coefficient between the reference model (REF) and the modified model (MDF) is shown in Table 3. The modified model achieved a 13.4% reduction in the total resistance coefficient, along with a 15.5% reduction in the pressure resistance component. The results of the modification studies reveal that the modified model provides considerable reductions in total resistance. The reduction in resistance is generally considered important, as it also directly affects wake characteristics (Hamed, 2022; Nazemian & Ghadimi, 2022). The wave patterns of the reference and modified models were investigated as well to understand the causes of resistance reduction.

Table 3. Total resistance coefficient values for reference model and modified model

	Reference Model	Modified Model
Total Resistance Coefficient ($C_T \times 10^3$)	7.984	6.914

The pressure coefficient distribution on the reference and modified models at a cruising speed of 4.12 m/s, corresponding to a Froude number of 0.38, is shown in Figure 5. The pressure coefficient distribution results reveal that there is a significant reduction in high-pressure values in the stern regions where improvements were applied in the modified model (MDF). The maximum pressure coefficient in the stern regions decreases from 0.75 in the reference model to 0.56 in the modified model. The modified model shows a uniform pressure distribution in the lower stern region. The reduction in pressure values and their smoother distribution are expected to result in a decrease in the amplitude and intensity of radiated waves from the stern regions.

Figure 6 provides a comparative analysis of the reference and modified models, focusing on wave transition and propagation, wave amplitude, and the formation of shoulder and stern waves. It is noted that a smoother wave transition is observed in the modified form. The modified model features more regular wave propagation and less pronounced stern and shoulder waves, contributing to smoother flow separation and reduced turbulence. A noticeable decrease in wave amplitude

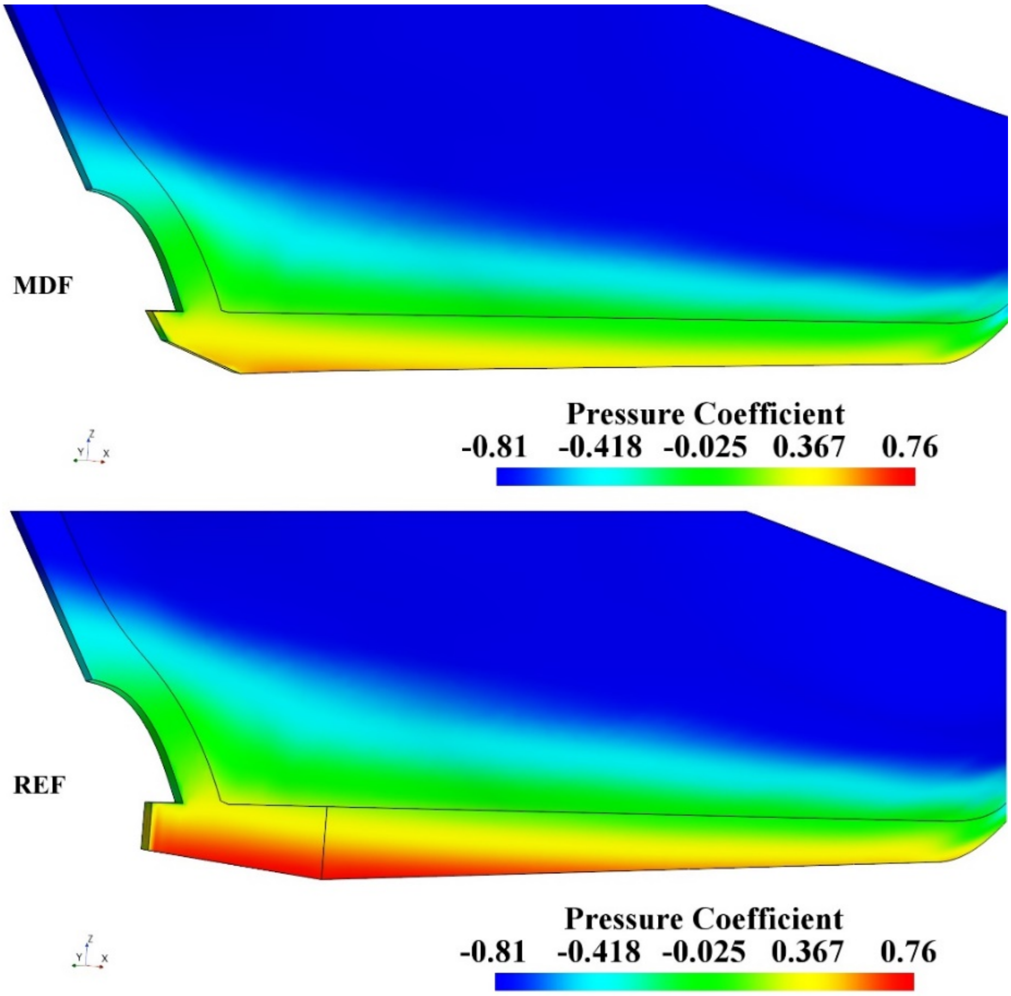

Figure 5. Pressure coefficient distribution of the reference and modified models

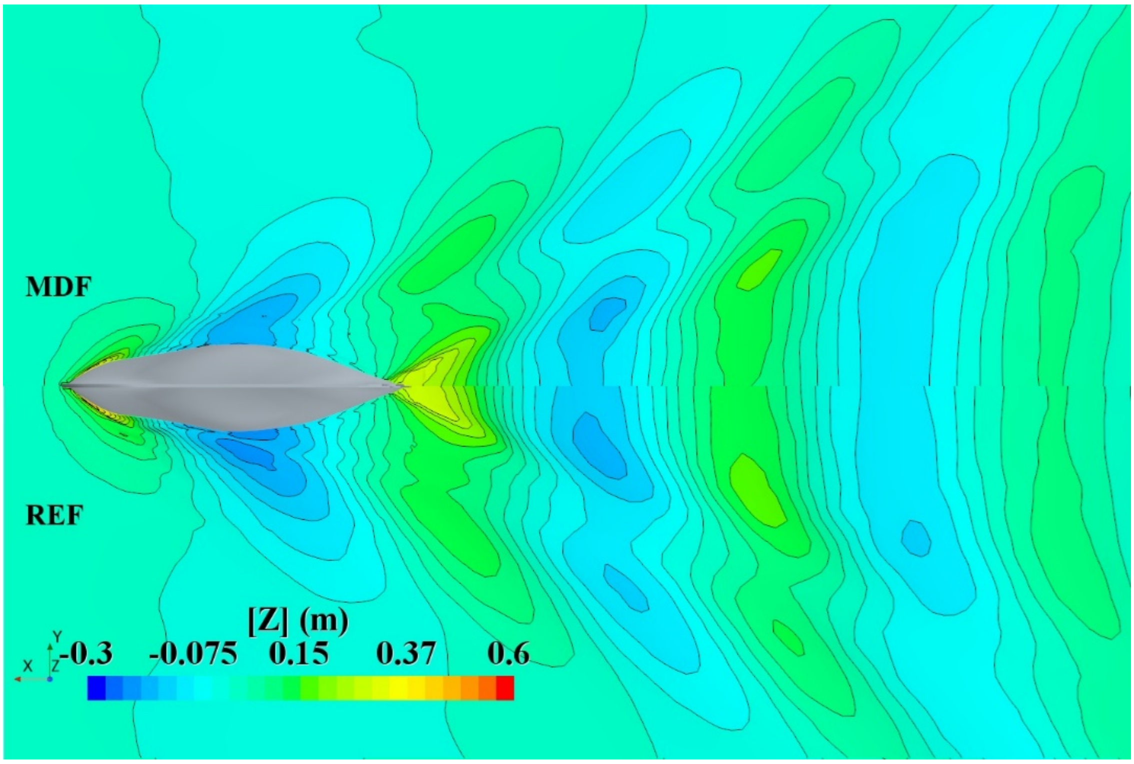

Figure 6. Wave pattern comparison between the reference (REF) and modified models (MDF)

by approximately 0.04 m is observed in the lower stern regions of the modified model. The decrease in wave amplitudes means that the water around the hull moves with less energy, resulting in a reduction in total resistance (Hamed, 2022; Nazemian & Ghadimi, 2022). It can be observed that the modified model experiences a reduction or cancellation of shoulder and stern waves compared to the reference model. The wave pattern improvements result in enhanced flow stability and reduced wave resistance, which in turn lead to better hydrodynamic performance and lower energy consumption for the modified model (Tezdogan et al., 2018; Hamed, 2022; Nazemian & Ghadimi, 2022).

Conclusion

A detailed investigation was conducted in this study to improve the hydrodynamic performance of a Tirhandil yacht by modification efforts on the stern region. The design of the reference and modified models was performed using CAD systems. The hydrodynamic characteristics of the reference Tirhandil model were determined through CFD analyses, and it was then concluded that form improvement efforts should focus on the stern region. The modification process was performed considering constraints on the design variables in the stern region and the main dimensions of the reference model. Various grid structures were analyzed in a grid independence study to determine the most suitable mesh configuration for the numerical analyses. In the numerical analyses, the SST k-Omega turbulence model was applied to simulate the turbulence around the hull form.

The reference model (REF) and the modified model (MDF) were comparatively investigated in terms of hydrodynamic characteristics. It was revealed that the modified model provided a 13.4% decrease in the total resistance coefficient and a 15.5% reduction in the pressure resistance component. The distribution of pressure coefficients indicates that high-pressure values were reduced in the stern region where improvements were implemented in the modified model (MDF). The maximum value of the pressure coefficient in the stern regions was decreased from 0.75 in the reference model to 0.56 in the modified model. The modified model features more regular wave propagation and experiences a reduction or cancellation of both shoulder and stern waves compared to the reference model. In the lower stern regions of the modified model, a significant decrease in wave amplitude of about 0.04 m is detected.

The literature review shows that there has been no previous study on improving hydrodynamic performance specifically in the stern region of Tirhandil yachts. This study presents a pioneering approach through the development of a unique Tirhandil hull design, with advanced hydrodynamic characteristics. This research also offers a framework for guiding future form optimization studies on sailing yachts. In future studies, the hydrodynamic characteristics of the hull form could be improved even more by applying form modification approaches to various regions of the hull form. Furthermore, similar research could be extended to consider harsh water conditions.

Acknowledgements

This research is supported by the Scientific and Technological Research Council of Türkiye (TÜBİTAK) under Project Number 223M093 within the framework of the project titled "Determination of Design Criteria and Form Optimization for Turkish Type Tirhandil Boats".

Compliance With Ethical Standards

Conflict of Interest

The author declares that there is no conflict of interest.

Ethical Approval

For this type of study, formal consent is not required.

Funding

Not applicable.

Data Availability

All data generated or analysed during this study are included in this published article.

References

Ali, B., & Ali, L. (2016). A new concept for the design of the shape ship stern. *Global Journal of Information Technology,* *6*(1), 18–26. https://doi.org/10.18844/gjit.v6i1.385

Anggriani, A. D. E., & Baso, S. (2020). Investigating the performance of a ship by matching the stern hull form to propeller and engine power. *EPI International Journal of Engineering,* *3*(2), 154–159. https://doi.org/10.25042/epi-ije.082020.11

Baso, S., Mutsuda, H., & Doi, Y. (2019). Predicting the motions of a fishing boat caused by improving the stern part using a hybrid particle-grid scheme. *International Journal of Technology,* *10*(2), 236-246. https://doi.org/10.14716/ijtech.v10i2.2354

Boussinesq, J. (1877). *Essai sur la theorie des eaux courantes.* Memoires presentes par divers savants a l'Academie des Sciences de l'Institut National de France. Tome XXIII, No 1. Imprimerie Nationale, Paris, France.

Celik, I. B., Ghia, U., Roache, P. J., & Freitas, C. J. (2008). Procedure for estimation and reporting of uncertainty due to discretization in CFD applications. *Journal of Fluids Engineering-Transactions of the ASME, 130*(7), 078001. https://doi.org/10.1115/1.2960953

Damianidis, K. (1989). *Vernacular Boats and Boatbuilding in Greece.* [Ph.D. Thesis, University of St. Andrews].

Deng, R., Chen, S. Y., Wu, T. C., Luo, F. Q., Jiang, D. P., & Li, Y. L. (2020). Investigation on the influence induced by interceptor on the viscous flow field of deep-sea vessel. *Ocean Engineering, 196*, 106735. https://doi.org/10.1016/j.oceaneng.2019.106735

Duy, T. N., & Hino, T. (2015). A study on the stern shape optimization of a container ship using Navier-Stokes analysis. *Journal of the Japan Society of Naval Architects and Ocean Engineers, 22*, 1–13. https://doi.org/10.2534/jjasnaoe.22.1

Ganos, G., & Loukakis, T. (1986). *Resistance characteristics of the trehantiri type boat.* Report of Research Group: Ship Hydromechanics and Structures (Mechanical, Maritime and Materials Engineering), Delft University of Technology, Netherlands.

Gencer, A. I. (2001). *Bahriye'de Yapılan Islahat Hareketleri ve Bahriye Nezareti'nin Kuruluşu (1789 - 1867).* Turkish Historical Society Publications.

Gür, M. C. (2020). *Kürekten Yelkene Kaybolan Miras.* Koç University Press.

Hamed, A. (2022). Multi-objective optimization method of trimaran hull form for resistance reduction and propeller intake flow improvement. *Ocean Engineering, 244*, 110352. https://doi.org/10.1016/j.oceaneng.2021.110352

ITTC. (2011). *Practical guidelines for ship CFD applications.* 26th ITTC Specialist Committee on CFD in Marine Hydrodynamics.

ITTC. (2014). *Practical guidelines for ship CFD applications.* 27th ITTC Specialist Committee on CFD in Marine Hydrodynamics.

Karafiath, G. (2012). Stern end bulb for energy enhancement and speed improvement. *Journal of Ship Production and Design, 28*(04), 172–181. https://doi.org/10.5957/JSPD.28.4.120050

Kükner, A., & Mamur, M. F. (2016). The effect of resistance on bow and stern forms. *Proceedings of the 1st International Congress on Ship and Marine Technology*, Türkiye, pp. 349-374.

Lena, C., Bonci, M., & van Walree, F. (2021). Effect of stern appendages configurations on the course-keeping of ships in stern-quartering seas. *International Shipbuilding Progress, 68*(1-2), 3–31. https://doi.org/10.3233/ISP-201006

Lu, Y., Chang, X., Yin, X., & Li, Z. (2019). Hydrodynamic design study on ship bow and stern hull form synchronous optimization covering whole speeds range. *Mathematical Problems in Engineering, 2019*(1), 2356369. https://doi.org/10.1155/2019/2356369

Mahmuzlu, E. (2019). Ottoman-Flagged Ships, 1830s-1860s: Hull, Rig, and Geography. *Drassana: revista del Museu Marítim, 27*, 120-168. https://doi.org/10.17561/dra.27.369256

Maki, A., Arai, J., Tsutsumoto, T., Suzuki, K., & Miyauchi, Y. (2016). Fundamental research on resistance reduction of surface combatants due to stern flaps. *Journal of Marine Science and Technology, 21*, 344–358. https://doi.org/10.1007/s00773-015-0356-8

Mansoori, M., & Fernandes, A. C. (2016). The interceptor hydrodynamic analysis for controlling the porpoising instability in high-speed crafts. *Applied Ocean Research, 57*, 40–51. https://doi.org/10.1016/j.apor.2016.02.006

Mansoori, M., & Fernandes, A. C. (2017). Interceptor and trim tab combination to prevent interceptor's unfit effects. *Ocean Engineering, 134*, 140–156. https://doi.org/10.1016/j.oceaneng.2017.02.024

Marcu, O., & Robe-Voinea, E. G. (2024). Stern flow hydrodynamics around a self-propelled maneuvering VLCC ship. *Engineering, Technology & Applied Science Research, 14*(4), 15283–15290. https://doi.org/10.48084/etasr.7624

Masuya, T. (2007). Hull form improvement of fishing vessels from the view point of seaworthiness. *Fisheries Engineering (Japan), 43*(3), 193-199.

Menter, F. R. (1994). Two-equation eddy-viscosity turbulence models for engineering applications. *AIAA Journal, 32*(8), 1598–1605. https://doi.org/10.2514/3.12149

Mutsuda, H., Ishida, A., Baso, S., & Doi, Y. (2013). Numerical investigation of resistance reduction of fishing boat by improving stern part. *Advanced Shipping and Ocean Engineering, 2*(3), 77–83.

Nazemian, A., & Ghadimi, P. (2022). Multi-objective optimization of ship hull modification based on resistance and wake field improvement: Combination of adjoint solver and CAD-CFD-based approach. *Journal of the Brazilian Society of Mechanical Sciences and Engineering, 44*, 1–27. https://doi.org/10.1007/s40430-021-03335-4

Ozen, S. (2017). *Gemiler Sözlüğü*. Denizler Publishing.

Solak, H. P. (2020). Multi-dimensional surrogate based aft form optimization of ships using high fidelity solvers. *Brodogradnja, 71*(1), 85–100. https://doi.org/10.21278/brod71106

Song, K. W., Guo, C. Y., Gong, J., Li, P., & Wang, L. Z. (2018). Influence of interceptors, stern flaps, and their combinations on the hydrodynamic performance of a deep-vee ship. *Ocean Engineering, 170*, 306–320. https://doi.org/10.1016/j.oceaneng.2018.10.048

Song, K., Gong, J., Ma, J., Xu, Q., Shi, Y., & Xu, F. (2024). Numerical study on the influence of interceptor and stern flap on ship resistance and motion response in regular waves. *Journal of Marine Science and Engineering, 12*(6), 929. https://doi.org/10.3390/jmse12060929

StarCCM+ User Guide. (2023). *StarCCM+ version 2310*. SIEMENS simcenter.

Suastika, K., Hidayat, A., & Riyadi, S. (2017). Effects of the application of a stern foil on ship resistance: A case study of an Orela crew boat. *International Journal of Technology, 8*(7), 1266–1275. https://doi.org/10.14716/ijtech.v8i7.691

Tezdogan, T., Shenglong, Z., Demirel, Y. K., Liu, W., Leping, X., Yuyang, L., & Incecik, A. (2018). An investigation into fishing boat optimization using a hybrid algorithm. *Ocean Engineering, 167*, 204–220. https://doi.org/10.1016/j.oceaneng.2018.08.059

Turan, B. İ. (2022). *Tırhandil ve piyade tipi tekne formlarının tasarım ve mühendislik perspektifinden karşılaştırılması* [Comparison of tirhandil and piyade type boat forms from design and engineering perspectives]. *Journal of Marine and Engineering Technology*, *2*(2), 78-90.

Turan, B. İ. (2023). Guideline for preliminary design phase of trawler type yachts. *Marine Science and Technology Bulletin*, *12*(3), 312-321. https://doi.org/10.33714/masteb.1334052

Turan, B. I., & Akman, M. (2021). Modeling and comparison of Bodrum Gulets' hull forms with round and transom sterns. *Journal of ETA Maritime Science*, *9*(2), 120-129. https://doi.org/10.4274/jems.2021.09327

Turan, B. İ., Akman, M., & Bulut, S. (2024). A conceptual design framework for tirhandil type sailing yachts. *Ships and Offshore Structures, In press*, 1-12. https://doi.org/10.1080/17445302.2024.2398176

Turan, B. İ., Akman, M., & Özbey, T. (2021). Design comparison of Bodrum Gulets and tirhandils. *Proceedings of the 2nd International Congress on Ship and Marine Technology*, Türkiye, pp. 491-497.

Wilcox, D. C. (1988). Reassessment of the scale-determining equation for advanced turbulence models. *AIAA Journal*, *26*(11), 1299–1310. https://doi.org/10.2514/3.10041